dam world 2015
Second International Dam World Conference
PORTUGAL • LISBON • LNEC • April 21-24, 2015

Advanced numerical techniques for modeling tensile crack propagation in gravity dams

I. F. Dias[*], J. Oliver[†], J. V. Lemos[*] and O. Lloberas-Valls[†]

[*] Laboratório Nacional de Engenharia Civil (LNEC)
Av. do Brasil, 101, 1700-066 Lisboa, Portugal
e-mail: idias@lnec.pt

Keywords: Concrete gravity dams, Fracture, Computational material failure, Strong discontinuities, E-FEM, Crack-path field, Strain injection

Abstract. *Cracks propagating deep inside gravity dams can seriously affect their structural safety. Due to the potential catastrophic scenarios associated to the collapse of large concrete dams, it is a fundamental issue to realistically predict the eventual crack profiles and the ultimate structural resistance associated to the failure mechanisms.*

This work investigates tensile crack propagation in concrete gravity dams by using some new recently developed numerical techniques (crack-path field and strain injection techniques) [1-3] associated to a Rankine-type plasticity model. The work carefully addresses aspects related to mesh independence (mesh bias and stress locking), robustness, and computational cost, which are the main issues in material failure modeling. The numerical simulations presented in the paper show the advantages of the presented approach.

1 INTRODUCTION

Nowadays, structural safety of large dams remains a great concern due to the high potential risk associated to this kind of structures. A dam failure, followed by a sudden flood wave, can result in large life losses and in strong environmental and economic impacts as it was reported for several catastrophic failure cases [4, 5]. Historically, the main causes of significant dam failures are related to foundation defects (erosion, sliding on its rock foundation, etc.) [6-8]. Structural failures, when not directly caused by foundation movements, are less frequent but its importance should not be minimized in the design neither in the safety control of the dam. Due to the importance of these structures, it is a worldwide standard practice to monitor continually dams as a part of the safety control process [9], which supports afterwards the safety assessment and decision. On the other hand, quantifying realistically concrete dams safety factors is a complex engineering question that depends on a multiplicity of phenomena affecting the performance and resistance of the dam and its foundation.

† E.T.S. d'Enginyers de Camins, Canals i Ports, Technical University of Catalonia
International Center for Numerical Methods in Engineering (CIMNE)
Campus Nord UPC, Edifici C-1, c/Jordi Girona 1-3, 08034 Barcelona, Spain.

In this work attention is focused in crack propagation through the dam body. Cracks progressing deep inside gravity dams can seriously affect its structural safety. Computational failure analysis can be an effective tool for predicting, realistically, the eventual crack profiles and the ultimate structural resistance, allowing improved estimation of the structural safety factor.

The importance of computational methods for modeling concrete dams was soon recognized by some authors in the 1980s, which have used *linear elastic fracture mechanics* [10-14] to perform the first computational simulations of fracture in concrete dams. These authors argue that, due to the large scale of dams, the fracture process zone is small in front of the overall structure and therefore *linear elastic fracture mechanics* can be applicable with limited errors, since failure occurs in a brittle (or quasi-brittle) manner. On the other hand, other authors argue that, due the specific characteristics of dam concrete (that can have characteristic length up to 10 times greater than common concrete), the non-linear effects should not be neglected, even for large dams [15, 16].

Apart from this theoretical and important question, in the 1990s, nonlinear fracture analysis starts becoming further used for fracture modeling of concrete dams, in the finite elements framework. Depending on the manner that the de-cohesion process at the crack interface is modeled, two major descriptions were used:

1. In the c*ohesive* (or discrete) *approach* [17] [18] the non-linear mechanical behavior is described by introducing a traction separation law (relating the traction vector and the vector of displacement jump) along the surface where the de-cohesive process occurs (typically coincident with the element sides).
2. In the *continuum approach* [19, 20] the non-linear mechanical behavior at the interface is described by a standard stress-strain constitutive model equipped with softening such that strains tend naturally to concentrate in narrow bands (strain localization). Then the assumption consists in admitting that the displacement jump can be captured in a *smeared* manner throughout the localization band. The fact that this numerical phenomena can be observed by just introducing strain softening in a constitutive model (damage, plasticity, smeared cracked) made this approach widely used for modeling material failure.

In both approaches fracture energy plays a fundamental role in order to make results physically meaningful (ensuring correct energy dissipation and overcoming the mesh size dependence). Despite the simplicity of these approaches the main flaw of these methods is the spurious dependence on the mesh alignment. This issue is critical for the reason that different meshes can deliver different results, in terms either of the crack trajectory or in terms of the dissipated energy. The main consequences of mesh dependence phenomena are well documented in the literature, and consist, essentially, in two types of undesirable behavior:

- *Mesh bias flaws*: Refers to the spurious tendency of the crack to follow certain preferred direction related to the mesh alignment, i.e. the crack tends to propagate parallel to the element sides avoiding zigzagging. The main inconvenience of this dependence is that it can lead to unrealistic\unphysical failure mechanism with consequences also in the ultimate structural load carrying capacity, which may be over or under-estimated.
- *Stress locking flaws*: Refers to the lack of ability of finite elements to capture strain localization, in a one-element-with localization band, without spurious stress transfer to the neighboring elements. The principal inconvenient of stress locking is the extra dissipation that occurs in elements outside the localization

band which results in a stiffer behavior that leads to an overestimation of the ultimate structural load carrying capacity, which is not on the safety side.

The flaws of these "classical methods" have motivated large efforts from numerous authors for enhancing and developing new numerical methods to improve the failure analysis of general structures, e.g., [21-28]. However, so far, most of them have been assessed uniquely with academic benchmarks and few cases of real-life structures have been reported [29].

This work investigates tensile crack propagation in concrete gravity dams by using some new recently developed numerical techniques (crack-path field and strain injection techniques) [1-3] associated to a Rankine-type plasticity model. The considered methodology is implemented in the finite element framework using continuum constitutive models equipped with strain softening. It consists of a procedure to insert, in proper parts of the domain, specific strain fields (constant strain and discontinuous strain modes) that will enhance the performance of the underlying standard finite elements for capturing and propagating strain localization. The necessary data to inject the discontinuous displacement modes into the appropriated position inside the finite element is obtained by an auxiliary technique conceived to identify the crack path: the crack-path field technique.

The methodology enjoys the benefits of the intra-elemental methods, E-FEM [30] or X-FEM [22], for capturing complex propagating displacement discontinuities in coarse meshes, without resorting to global code invasive crack-path-tracking algorithms.

2 STRAIN INJECTION TECHNIQUES

Strain injection refers to a general numerical technique that consists in inserting, in selected parts of the domain and during different stages of the simulation, specific strain fields, that have the goal of enhancing the performance of classical finite elements. The key point of this technique is the split of the domain into two disjoint subdomains: the injection domain, $\mathcal{B}_{inj}$, where the enhanced strain modes are injected and the remaining part of the body where no improvement is intended (see Figure 1).

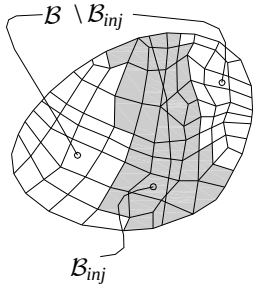

Figure 1 Discretized domain of typical size h.

Considering a finite element discretization and the domain split of Figure 1, the variational equation of the mechanical problem (equivalent to the virtual work principle) can be written as:

$$\underbrace{\int_{\mathcal{B}\setminus\mathcal{B}_{inj}} \nabla^s \boldsymbol{\eta}^h : \dot{\boldsymbol{\Sigma}}(\nabla^s \dot{\boldsymbol{u}}^h) d\mathcal{B}}_{\text{Standard term}} + \underbrace{\sum_{\forall \mathcal{B}^{(e)} \subset \mathcal{B}_{inj}(t)} \int_{\mathcal{B}^{(e)}} \nabla^s \boldsymbol{\eta}^h : \dot{\boldsymbol{\Sigma}}(\dot{\varepsilon}_{inj}^{(e)}) d\mathcal{B}}_{\text{Strain injection term}} = W^{ext}(\boldsymbol{\eta}, \dot{\mathbf{b}}, \dot{\mathbf{t}}^*) \quad \forall \boldsymbol{\eta}^h \qquad (1)$$

Where the work produced by the internal forces is computed by the sum of two terms. The first one, the standard term, corresponds to that part of the domain where no enhancement is done and, therefore, strains are computed directly from the symmetric gradient, ∇^s, of the

displacement field, $\boldsymbol{u}$ (compatibility equation), as it is done in standard displacement based finite element formulations. The second term, the strain injection term, corresponds to the part of the domain where a specific strain field, $\dot{\varepsilon}_{inj}^{(e)}$, is injected in the constitutive equation $\boldsymbol{\Sigma}(\bullet)$ of those elements belonging to the injection domain, $\mathcal{B}_{inj}(t)$. Here the strains are not computed from the compatibility equation, so, new equations defining the enhanced strain modes, $\dot{\varepsilon}_{inj}^{(e)}$, should be added to the system.

REMARK: It is out of the scope of this paper to provide full mathematical details of the strain injection technique. However, in order to provide the readers a general insight about the basis of the methodology, the main ideas and basic motivation of the techniques are briefly presented. In [1] a rigorous presentation of the technique and its implementation details can be consulted by interested readers. More information can also be found in [2, 3].

3 STRAIN INJECTION FOR FAILURE ANALYSIS

The domain split illustrated in Figure 1, and supported by equation (1), requires the definition of the strain injections modes, $\dot{\varepsilon}_{inj}^{(e)}$, and the injection domain, $\mathcal{B}_{inj}(t)$. This definition should be oriented to address the specific features and challenges of the problem we are dealing with. In the context of material failure modeling, the injected strain modes have the goal of enhancing the performance of classical finite elements in capturing strain localization.

3.1 Strain injection modes

In previous work of the authors [1], two strain fields were proposed to be injected in *quadrilateral elements*: the constant strain mode (CSM) and the discontinuous displacement mode (DDM).

3.1.1 The Constant Strain Mode (CSM)

The constant strain mode consists of assuming the strains constant within the quadrilateral finite element:

$$\Rightarrow \quad \dot{\varepsilon}_{inj}^{(e)} = \dot{\varepsilon}_{CSM}^{(e)} = \overline{\boldsymbol{\nabla}^s \dot{\boldsymbol{u}}^h}^{(e)} \qquad \forall \mathcal{B}^{(e)} \subset \mathcal{B}_{inj}(t) \tag{2}$$

In equation (2), the notation $\overline{(\cdot)}^{(e)}$ stands for the spatial average of $(\cdot)$ on the element (e).

The main goal of this injection is to provide extra flexibility to those finite elements that are amenable to develop discontinuities, therefore enhancing their propagation capabilities and avoid mesh bias dependences.

We would like to remark that, for the used quadrilateral elements, the proposed constant strain mode injection is equivalent to performing reduced integration of the standard displacement-based finite element formulation at the injected elements. The key difference between both methodologies is that the CSM is only used in very few elements (those belonging to the injection domain – typically the part of the body where the fracture is being processed) while reduced integration techniques are applied in the entire domain.

3.1.2 The Discontinuous-Displacement Mode (DDM)

The *Discontinuous-Displacement Mode* consists of enriching the element kinematics with the strong discontinuity kinematics [30] (summarized at Box 1) such that the mechanical behavior of the crack can be perfectly captured inside the finite element without spurious stress transfer to the neighboring elements (stress locking phenomena).

Strong discontinuity kinematics:

$$\dot{\varepsilon} = \underbrace{\boldsymbol{\nabla}^S \hat{\dot{\boldsymbol{u}}} - (\boldsymbol{\nabla}\varphi \otimes [\![\dot{\boldsymbol{u}}]\!])^S}_{\hat{\dot{\varepsilon}}\ (regular)} + \delta_{\mathcal{S}}\,(\mathbf{n} \otimes [\![\dot{\boldsymbol{u}}]\!])^S$$

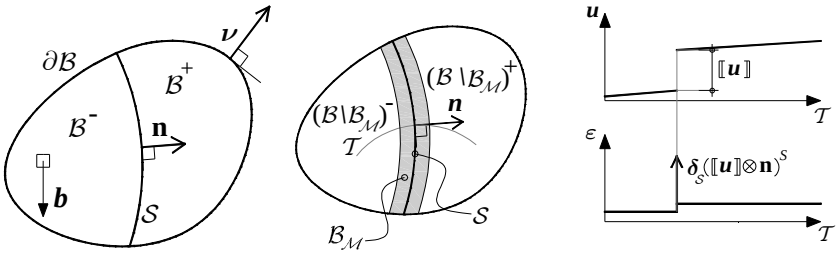

$\mathcal{S}$ - Discontinuity surface

$\mathbf{n}$ - Unit vector orthogonal to $\mathcal{S}$ (pointing to $\mathcal{B}^+$),

$[\![\dot{\boldsymbol{u}}]\!]$ - Strong discontinuity jump ($[\![\dot{\boldsymbol{u}}]\!] = \dot{\boldsymbol{u}}|_{\mathbf{x}\in(\partial\mathcal{B}^+\cap\mathcal{S})} - \dot{\boldsymbol{u}}|_{\mathbf{x}\in(\partial\mathcal{B}^-\cap\mathcal{S})}$)

$\delta_{\mathcal{S}}$ - Dirac distribution shifted to $\mathcal{S}$

$\varphi(\mathbf{x})$ - Continuous *indicatrix* function fulfilling: $\varphi(\mathbf{x}) = \begin{cases} 0 & \forall \mathbf{x} \in (\mathcal{B} \setminus \mathcal{B}_{\mathcal{M}})^- \\ 1 & \forall \mathbf{x} \in (\mathcal{B} \setminus \mathcal{B}_{\mathcal{M}})^+ \end{cases}$

Box 1 Summary of the strong discontinuity kinematics (see [21]).

Inspired in the strong discontinuity kinematics, an element-wise constant discontinuous-displacement mode was proposed:

$$\dot{\varepsilon}^{(e)}_{inj} = \dot{\varepsilon}^{(e)}_{DDM} = \overline{\nabla^S \hat{\dot{\boldsymbol{u}}}^h}^{(e)} - (\overline{\nabla\varphi^h}^{(e)} \otimes [\![\dot{\boldsymbol{u}}]\!]^{(e)})^S + \delta^{k,(e)}_{\mathcal{S}} ([\![\dot{\boldsymbol{u}}]\!]^{(e)} \otimes \mathbf{n}^{(e)})^S \quad \forall \mathcal{B}^{(e)} \in \mathcal{B}_{inj}(t) \tag{3}$$

3.2 Injection domains

After defining the strain modes to inject, the subsequent questions to be posed are *where* and *when* these strain modes should be injected in order to effectively improve the performance of classical finite elements for capturing strain localization. The answer to these questions is given by selecting proper injection domains. In the context of material failure modeling it is intuitively reasonable that the proposed strain modes should be injected in that part of the body where the fracture is being processed. By this reason the definition of the injection domains $\mathcal{B}_{inj}(t)$ is grounded on consistent mechanical criteria, such as the *discontinuous bifurcation analysis* that qualifies a stress/strain state as compatible with the onset of a discontinuous displacement field.

The *injection domain*, $\mathcal{B}_{inj}$, is that part of the domain where several strain mode injections can be performed (it has common conditions for all possible injections). In the preceding section two strain modes were proposed: the CSM and the DDM. Therefore two sub-domains of $\mathcal{B}_{inj}$ ($\mathcal{B}_{loc}$ and $\mathcal{B}_{dis}$) where these strain modes are respectively injected must be defined, such that: $\mathcal{B}_{inj}(t) = \mathcal{B}_{loc}(t) \cup \mathcal{B}_{dis}(t)$:

- the injection domain, $\mathcal{B}_{inj}(t)$, contains all the bifurcated elements which are in loading condition at the current time t.
- the discontinuity domain, $\mathcal{B}_{dis}(t)$, contains all the elements that have bifurcated and, in addiction, are effectively developing a strain localization process. Notice that not all the bifurcated elements develop cracks; some of the elements initially bifurcated unload elastically in subsequent time steps. In order to successfully determine this

domain, the discontinuity path should be identified in advance. In the context of the strain injection techniques this is done by the Crack-Path Field technique.

- the localization domain $\mathcal{B}_{loc}(t)$ includes all the in-loading bifurcated elements (belonging therefore to the injection domain) which do not verify, yet, the conditions for belonging to the discontinuity domain, i.e.: $\mathcal{B}_{loc}(t) = \mathcal{B}_{inj}(t) \setminus \mathcal{B}_{dis}(t)$.

All the injection domains can evolve very quickly over time. In fact, part of the elements that initially bifurcate, tend in a subsequent stage to unload elastically leaving, therefore, the injection domain, while others, crossed by the discontinuity, remain developing strain localization until being crossed by the discontinuity. In Figure 2, a typical load process is depicted.

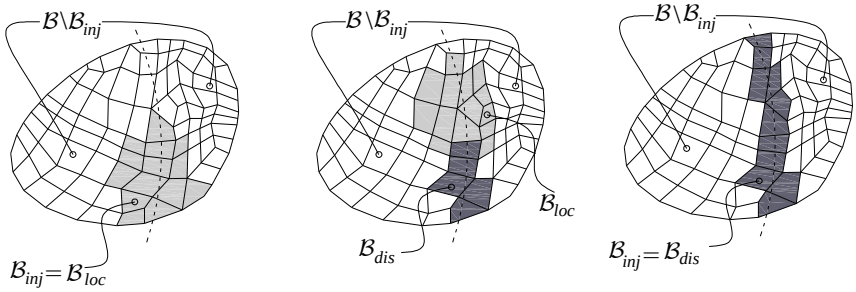

Figure 2 Evolution of the injection domains for three typical stages of loading.

3.3 Summary

With the definition of the strain modes and the respective injection domains in hand, equation (1) can be specified as follows:

$$\underbrace{\int_{\mathcal{B}\setminus\mathcal{B}_{inj}} \boldsymbol{\nabla}^s\boldsymbol{\eta}^h : \dot{\boldsymbol{\Sigma}}(\boldsymbol{\nabla}^s\dot{\boldsymbol{u}}^h)d\mathcal{B}}_{\text{Standard term}} + \sum_{\forall\mathcal{B}^{(e)}\subset\mathcal{B}_{loc}(t)} \underbrace{\int_{\mathcal{B}^{(e)}} \boldsymbol{\nabla}^s\boldsymbol{\eta}^h : \dot{\boldsymbol{\Sigma}}(\dot{\varepsilon}^{(e)}_{CSM})d\mathcal{B}}_{\text{CSM injection}} + \sum_{\forall\mathcal{B}^{(e)}\subset\mathcal{B}_{dis}(t)} \underbrace{\int_{\mathcal{B}^{(e)}} \boldsymbol{\nabla}^s\boldsymbol{\eta}^h : \dot{\boldsymbol{\Sigma}}(\dot{\varepsilon}^{(e)}_{DDM})d\mathcal{B}}_{\text{DDM injection}} = +W^{ext}(\boldsymbol{\eta},\dot{\mathbf{b}},\dot{\mathbf{t}}^*) \quad \forall\,\boldsymbol{\eta}^h \in \mathcal{V}_0^h \tag{4}$$

where the strain modes to inject, $\dot{\varepsilon}^{(e)}_{CSM}$ and $\dot{\varepsilon}^{(e)}_{DDM}$, are defined by means of expression (2) and (3) respectively. Equation (4) summarizes how the internal forces work is computed at each injection domain of Figure 2.

4 REPRESENTATIVE NUMERICAL SIMULATION: A GRAVITY DAM MODEL

Carpinteri et al. [31] have tested experimentally scale-down models of a gravity dam. The models have a horizontal notch on the upstream side and the experimental test was driven by controlling the crack mouth opening at that notch. Figure 3 illustrates the experiment setup, including the model dimensions, the position of the notch and the equivalent hydraulic loads. The finite element mesh and mechanical properties used in the numerical model are also shown in this figure.

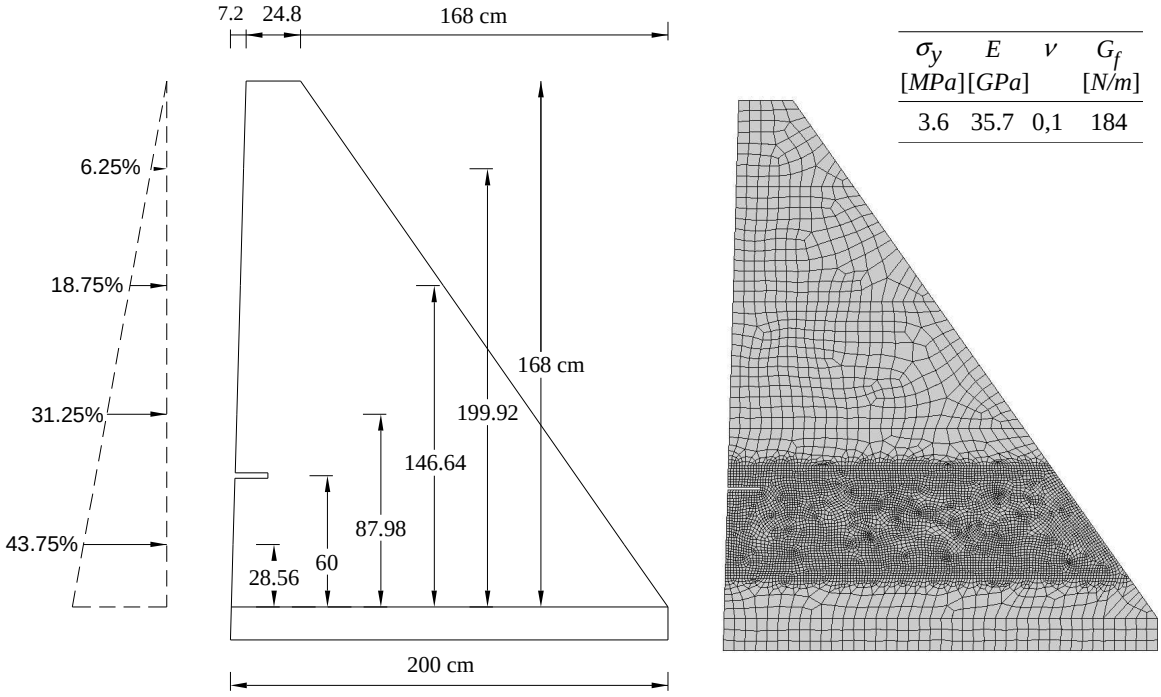

σ_y [MPa]	E [GPa]	ν	G_f [N/m]
3.6	35.7	0,1	184

Figure 3 Dam model; finite element mesh; mechanical properties used in the numerical model, being σ_y the yielding stress, E the Young's modulus, ν the Poisson's ratio and G_f the fracture energy.

In the numerical simulations, the loading process was performed by applying, in a first stage, the self-weight loads and, in a second stage, the hydraulic loads. The second stage is carried out through a step by step Newton-Raphson scheme in which the crack mouth displacement at the notch is controlled by using arc-length techniques.

The material behavior was simulated by using a Rankine-type plasticity [2, 3, 32] model that allows modeling fracture opening in mode I. By reasons of robustness, that is a very important issue when modeling material failure, an IMPLEX scheme [33] for the integration of the constitutive equation was used.

In Figure 4 quantitative responses for three different options are depicted in terms of the force–CMOD (Crack-Mouth-Opening Displacement) curves. The "strain injection" curve was obtained by using the strain injection techniques described in this work, while the "experimental" and "cohesive model curves" were obtained by Carpinteri et al, being the former experimentally measured and the later numerically computed by using a cohesive crack model supported in an automatic remeshing processes, at each crack grow step, so that the crack lies in the finite element mesh sides.

It can be observed an excellent agreement between both numerical solutions. The obvious advantage of the strain injection technique is that no remeshing process is needed. Relatively, to the comparison with the experimental solution, it is noticed some level of discrepancy in terms of the post peak behavior, which is more dissipative for the experimental case. That might be attributed to some issues of the experimental set-up that are missed in the numerical modeling.

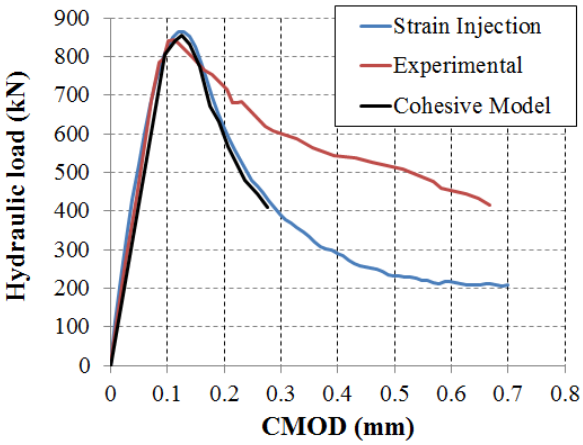

Figure 4 Force displacement curves: hydraulic load versus Crack Mouth Opening Displacement (CMOD).

In terms of crack propagation patterns, Figure 5 shows a good agreement between the experimental and the numerical results obtained with the strain injection techniques. Finally, Figure 6 shows the deformed configuration and the crack path at the final stage of loading.

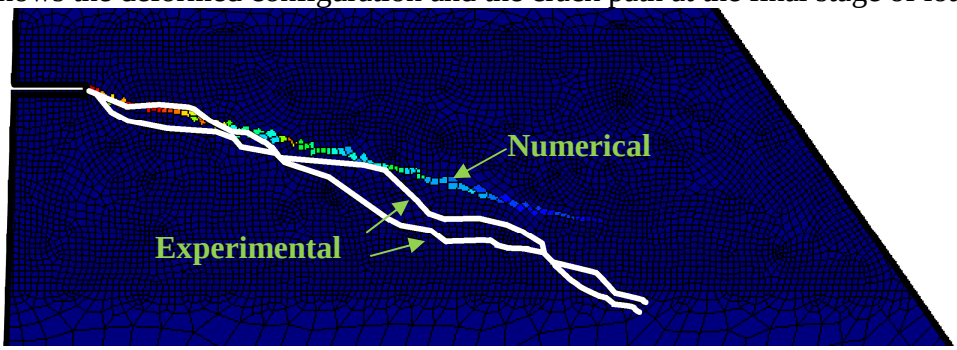

Figure 5 Crack trajectories. The numerical solution crack pattern is plotted in terms of the equivalent plastic deformation. The experimental trajectories have been added to the figure through the white lines corresponding to both sides of the experimental 3d model.

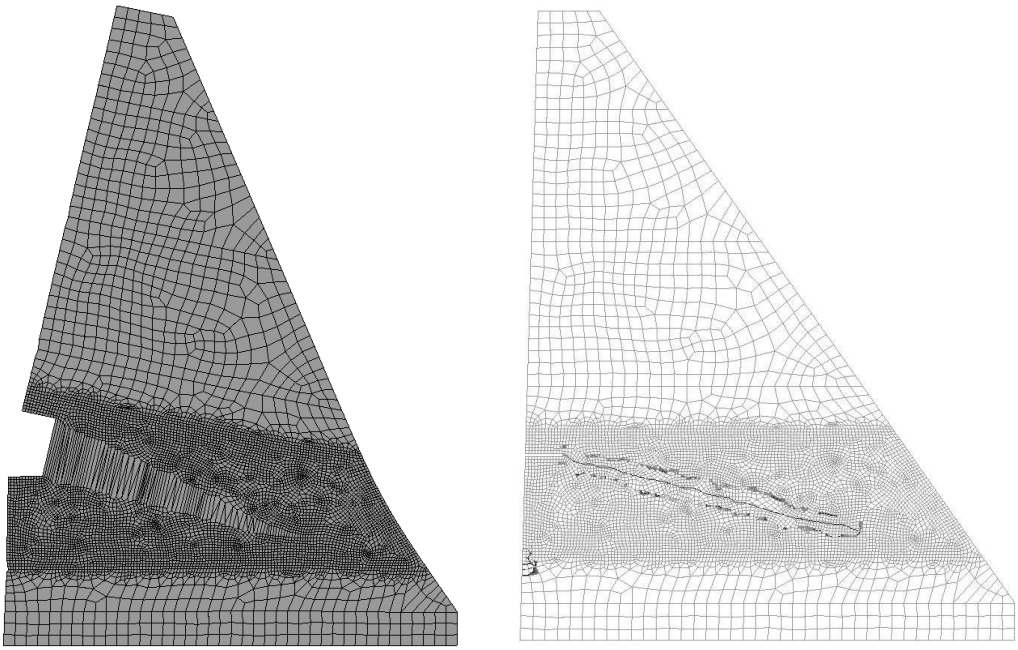

Figure 6 a) Deformed configuration; b) Crack path. Results obtained by the strain injection techniques at the final step of the computations.

4.1 Mesh dependency analysis

When modeling material failure, mesh dependence is a critical issue since different meshes can deliver different results, in terms either of the crack trajectory or in terms of the dissipated energy.

In order to access if the results obtained by using the injection techniques are mesh independent, comparative analysis were carried out by using two different meshes: one structured and another unstructured (Figure 7). Additionally, the obtained results are also compared with the ones coming from standard displacement-based (irreducible) formulations, which are known to suffer from mesh dependence.

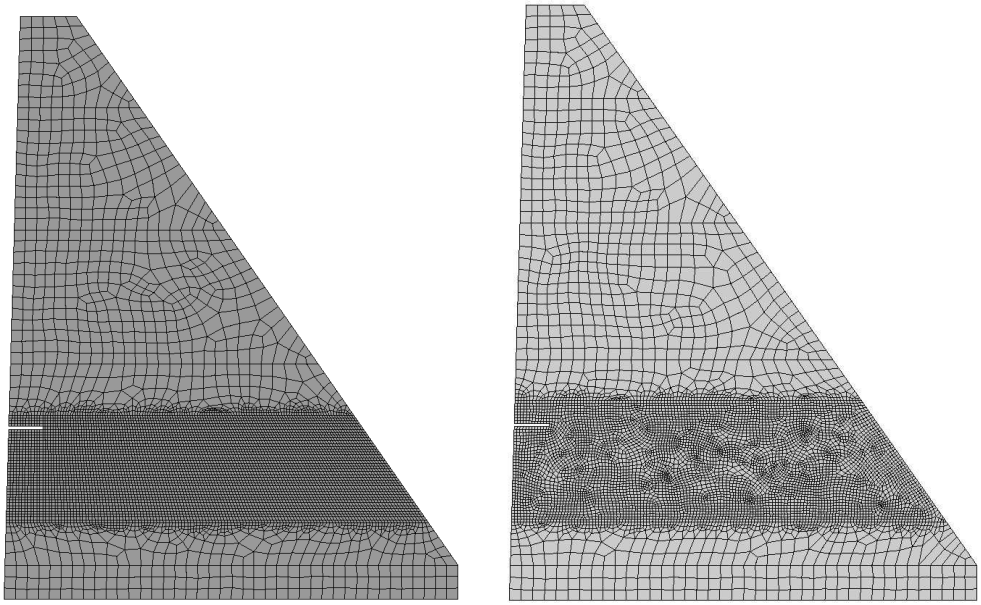

Figure 7 Finite element meshes; a) structured mesh, b) unstructured mesh.

Figure 8 compares results obtained with the two finite element formulations (strain injection techniques and irreducible formulation) for both meshes shown in Figure 7. Since the Rankine constitutive model is the same for both formulations, the differences shown in Figure 8 can be only attributed to the performance of the finite element formulation.

In fact, the results obtained with the irreducible formulation show a considerably stiffer behavior in terms of the post-peak response that can be related to spurious extra energy dissipation due to stress locking defects. This issue has also consequences in the peak load which is miss-predicted for the irreducible formulation when using the unstructured mesh. Although, for this specific example, the differences in terms of the peak load are not too large (less than 10%), we would like to remark that the results obtained with the irreducible formulation are not in the safety side, since the structure can fail due to lower hydraulic load, as it is predicted by the strain injection techniques.

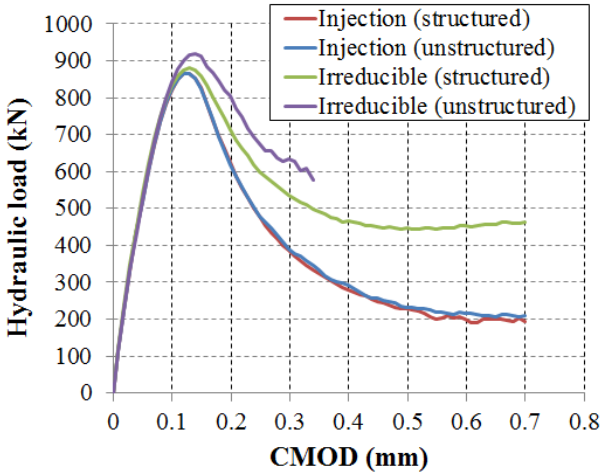

Figure 8 Finite element meshes; a) structured mesh, b) unstructured mesh.

It is also remarkable that results obtained by strain injection technique, for both meshes, are near the same. This can be appreciated either by the overlapping curves of Figure 8 or by the near coincident crack trajectories of Figure 9.

The results shown in Figure 8 and Figure 9 by the strain injection techniques are strong indicators of their independence relatively to the finite element mesh.

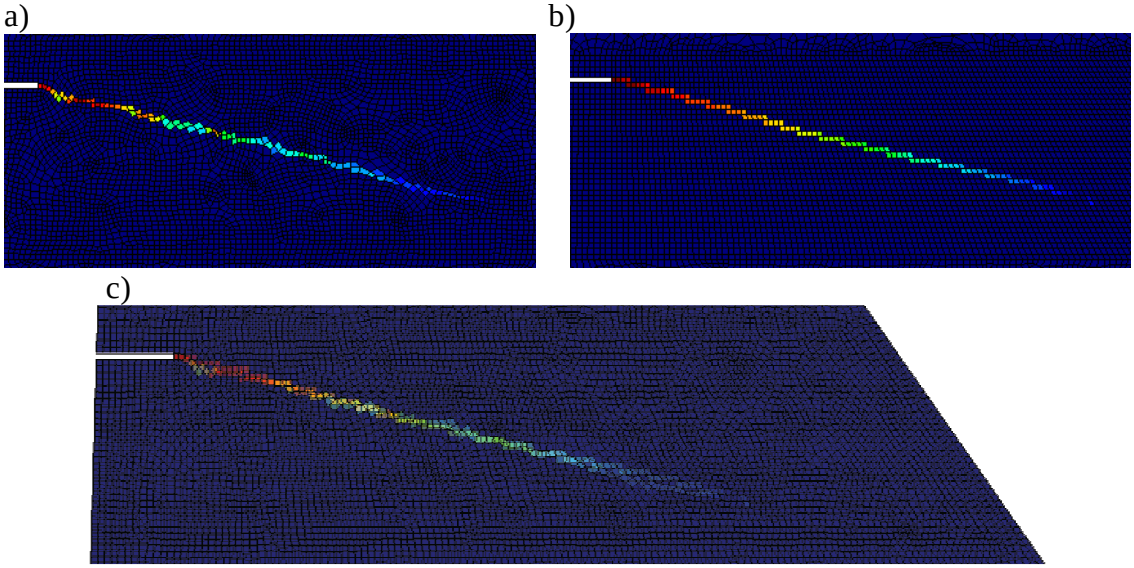

Figure 9 Crack patterns plotted in terms of the equivalent plastic strain. Results obtained by using the strain injection techniques. a) Unstructured; b) Structured mesh; c) overlap of results obtained with both meshes.

Relatively to the results obtained by the irreducible formulation, Figure 10 shows different results in terms of the crack patterns. This issue is related to the mesh bias dependence since the crack pattern obtained for the structured mesh seems to be clearly influenced by horizontal mesh directions.

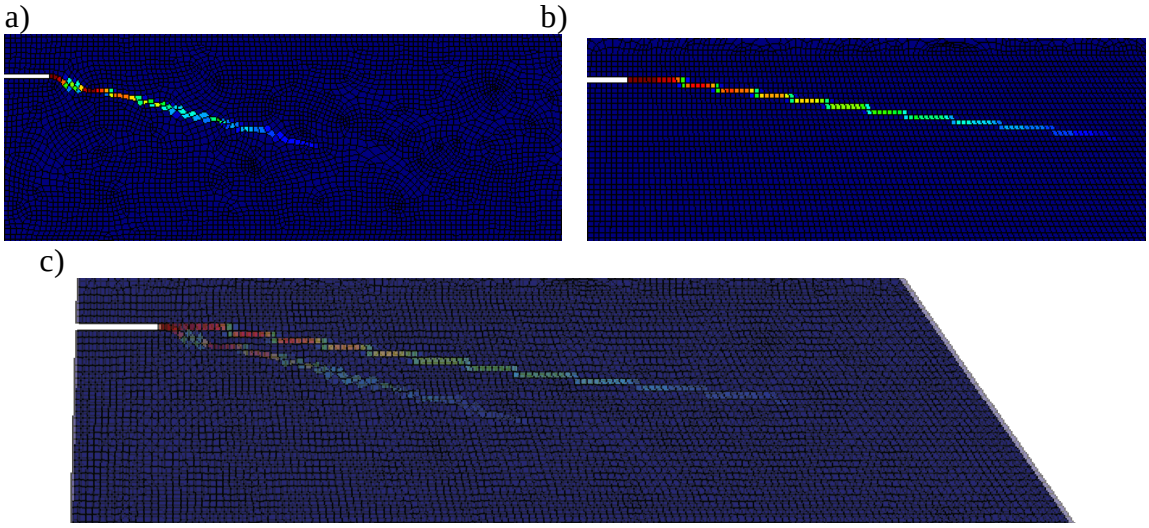

Figure 10 Crack pattern plotted in terms of the equivalent plastic deformation. Results obtained by using the irreducible formulation. a) Unstructured; b) Structured mesh; c) overlap of results obtained with both meshes.

5 CONCLUSIONS

In this work the potential of the recently proposed strain injection techniques, so far with applications limited to some academic benchmarks, has been explored for studying crack propagation in gravity concrete dams.

The results show clearly, the improvements obtained by using the new methodology in terms of mesh independence, either avoiding mesh bias or stress locking effects. This spurious undesirable behavior can lead to unrealistic failure mechanisms or to the overestimation of the ultimate structural load carrying capacity. In the numerical simulation, the displacement based classical formulation delivers results overestimating the structural resistance in about 10%, which is not on the safety side.

The new methodology has several advantages that the authors would like to remark:

- Mesh independence.
- Low computational cost – the explored approach captures the crack inside the finite element, which means that coarse meshes can be used when compared with the finer meshes required by other methodologies (nonlocal [25, 26], phase field [23], etc.) that use several elements across the band for modeling the crack. Moreover, all the additional degrees of freedom (related to the enhanced strain modes) are condensed out at the element level. The final result is a methodology that keeps the computational cost at the level of the standard displacement-based finite element formulations.
- Noninvasive numerical implementation - The strain-injection technique in combination with the crack-path-field technique, avoids the code invasive global crack tracking algorithms, usually used in association with other intra-elemental approaches (E-FEM [21] or X-FEM [22]), with no apparent cost in terms of robustness. This issue is a strong advantage, since the implementation tasks in a non-linear finite element code, affects, essentially, the element level.
- Generality – in the sense that the method affects exclusively the finite element formulation, this meaning that it can be used, in principle, with any continuum constitutive model equipped with strain softening.

The strain injection techniques are, due to these important properties that address the main issues of material failure modeling (mesh independence, computational cost, robustness), a methodology particularly efficient for modeling tensile crack propagation in concrete dams. Moreover, the results obtained in this paper show that the method is ready for being used in practice, allowing improved estimation of the structural safety factor and helping in the security control of those gravity concrete dams which might be particularly vulnerable for crack propagation.

The ongoing extension of the presented methodology to 3D cases will open the application field to large arch dams.

ACKNOWLEDGMENTS

This work was partially supported by the European Research Council under the Advanced Grant: ERC-2012-AdG 320815 COMP-DES-MAT “Advanced tools for computational design of engineering materials”.

Oriol Lloberas-Valls gratefully acknowledges the funding received from the Spanish Ministry of Economyand Competitiveness through the "Juan de la Cierva" Postdoctoral Junior Grant: JCI-2012-13782.

REFERENCES

[1]. Oliver, J., Dias, I.F., and Huespe, A.E., Crack-path field and strain-injection techniques in computational modeling of propagating material failure. *Computer Methods in Applied Mechanics and Engineering*, 2014. **274**(0): p. 289-348.

[2]. Dias, I.F., *Crack Path Field and Strain Injection Techniques in Numerical Modeling of Propagating Material Failure*. 2012, Ph.D. Thesis. Universitat Politècnica de Catalunya: (BarcelonaTech/UPC), Barcelona, Spain.

[3]. Dias, I.F., Oliver, J., and Huespe, A.E., *Strain Injection Techniques in Numerical Modeling of Propagating Material Failure*, in *Monograph CIMNE Nº-134*. 2012, International Center for Numerical Methods in Engineering: Barcelona. http://www.cimne.com/compdesmat/cvdata/cntr1/dtos/img/mdia/Downloads/M134.pdf.

[4]. Anderson, C., Mohorovic, C., Mogck, L., Cohen, B., and Scott, G., *Concrete Dams : Case Histories of Failures and Nonfailures with Back Calculations*. 1998: U.S. Department of Interior, Bureau of Reclamation, Dam Safety Office.

[5]. Charles, J.A., Tedd, P., and Warren, A., *Lessons from Historical Dam Incidents: Technical Summary*. 2011: Environment Agency.

[6]. CSED, C.o.S.o.E.D., *Safety of Existing Dams:Evaluation and Improvement*. 1983: The National Academies Press.

[7]. ICOLD, I.C.o.L.D., *Lessons from dam incidents*. Complete ed ed. 1974, Pari: ICOLD.

[8]. Strom, R.W., Cunningham, G., and Safety, I.C.o.D., *Training Aids for Dam Safety: Evaluation of Concrete Dam Stability*. 1990: U.S. Government Printing Office.

[9]. ICOLD, I.C.o.L.D., *Monitoring of dams and their foundations. State of the art. Bulletin number 68.* 1989, Paris: ICOLD.

[10]. Saouma, V.E., Ayari, M.L., and Boggs, H. *Fracture Mechanics of Concrete Gravity Dams*. in *SEM/RILEM International Conference on Fracture of Concrete Rock*. 1987. Houston, Texas,.

[11]. Chappell, J., Ingraffea, F., and R., C.A., *A fracture mechanics investigation of the cracking of Fontana Dam*. Report 81-7. 1981, Ithaca, New York: Cornell University, Department of Structural Engineering, School of Civil and Environmental

Engineering.
[12]. Linsbauer, H.N. *Fracture mechanics models for characterizing crack behaviour of gravity dams*. in *Proceedings of the 15th ICOLD*. 1985. Lausanne.
[13]. Gioia, G., Bazant, Z.P., and Pohl, B.P., Is no-tension dam design always safe. *Dam Engineering*, 1992. **3**: p. 23-34.
[14]. Plizzari, G., LEFM Applications to Concrete Gravity Dams. *Journal of Engineering Mechanics*, 1997. **123**(8): p. 808-815.
[15]. Brühwiler, E. and Wittmann, F.H., Failure of dam concrete subjected to seismic loading conditions. *Engineering Fracture Mechanics*, 1990. **35**(1–3): p. 565-571.
[16]. Bhattacharjee, S. and Léger, P., Application of NLFM Models to Predict Cracking in Concrete Gravity Dams. *Journal of Structural Engineering*, 1994. **120**(4): p. 1255-1271.
[17]. Hillerborg, A., Modeer, M., and Petersson, P.E., Analysis of crack formation and crack growth in concrete by means of fracture mechanics and finite elements. *Cement and concrete research*, 1976. **6**(6): p. 773-782.
[18]. Dugdale, D.S., Yielding of steel sheets containing slits. *Journal of the Mechanics and Physics of Solids*, 1960. **8**(2): p. 100-104.
[19]. Rots, J.G., *Computational Modeling of Concrete Fracture*. 1988, Delft University of Technology.
[20]. Rashid, Y., Analysis or prestressed concrete pressure vessels. *Nuclear Engineering and Design* 1968. **7**: p. 773-782.
[21]. Oliver, J. and Huespe, A.E., Continuum approach to material failure in strong discontinuity settings. *Computer Methods in Applied Mechanics and Engineering*, 2004. **193**(30-32): p. 3195-3220.
[22]. Belytschko, T., Moes, N., Usui, S., and Parimi, C., Arbitrary discontinuities in finite elements. *International Journal for Numerical Methods in Engineering*, 2001. **50**(4): p. 993-1013.
[23]. Miehe, C., Welschinger, F., and Hofacker, M., Thermodynamically consistent phase-field models of fracture: Variational principles and multi-field FE implementations. *International Journal for Numerical Methods in Engineering*, 2010. **83**(10): p. 1273-1311.
[24]. Francfort, G.A. and Marigo, J.J., Revisiting brittle fracture as an energy minimization problem. *Journal of the Mechanics and Physics of Solids*, 1998. **46**(8): p. 1319-1342.
[25]. Pijaudier Cabot, G. and Bazant, Z., Nonlocal damage theory. *Journal Engineering Mechanics ASCE*, 1987. **113**: p. 1512-1533.
[26]. de Borst, R. and Mühlhaus, H.-B., Gradient-dependent plasticity: Formulation and algorithmic aspects. *International Journal for Numerical Methods in Engineering*, 1992. **35**(3): p. 521-539.
[27]. Saether, E., Yamakov, V., Phillips, D.R., and Glaessgen, E.H., *An Overview of the State of the Art in Atomistic and Multiscale Simulation of Fracture* NASA/TM-2009-215564, Editor. 2009.
[28]. Cervera, M., Chiumenti, M., and Codina, R., Mesh objective modeling of cracks using continuous linear strain and displacement interpolations. *International Journal for Numerical Methods in Engineering*, 2011. **87**(10): p. 962-987.
[29]. Jirásek, M. and Zimmermann, T., Rotating Crack Model with Transition to Scalar Damage. *Journal of Engineering Mechanics*, 1998. **124**(3): p. 277-284.
[30]. Simo, J., Oliver, J., and Armero, F., An analysis of strong discontinuities induced by strain-softening in rate-independent inelastic solids. *Computational Mechanics*, 1993. **12**: p. 277-296.

[31]. Carpintieri, A., Valente, S.V., Ferrara, G., and Imperato, A.L. *Experimental and Numerical Fracture Modelling of a Gravity Dam*. in *Fracture Mechanics of Concrete Structures*. 1992: Elsevier Appl. Sci.

[32]. Feenstra, P.H. and De Borst, R., A plasticity model and algorithm for mode-I cracking in concrete. *International Journal for Numerical Methods in Engineering*, 1995. **38**(15): p. 2509-2529.

[33]. Oliver, J., Huespe, A., Blanco, S., and Linero, D., Stability and robustness issues in numerical modeling of material failure with the strong discontinuity approach. *Computer Methods in Applied Mechanics and Engineering*, 2006. **195**(52): p. 7093-7114.